

Measurement of Cavitation Nuclei Dispersion in Hydrodynamic Facilities

Elizabeth S. C. Allan¹, Luka Barbaca^{1*}, Patrick S. Russell¹, James A. Venning¹, Bryce W. Pearce¹ and Paul A. Brandner¹

¹ Cavitation Research Laboratory, Australian Maritime College, University of Tasmania, Launceston, TAS 7250, Australia

*mailto: Luka.Barbaca@utas.edu.au

Abstract

Cavitation nuclei populations are characterized by a stochastic distribution, both in size and dispersion within the flow domain. In order to statistically characterize the nuclei spatial distribution, a volumetric measurement technique based on use of Mie-Scattering Imaging (MSI) has been developed. Spatial characterization of nuclei concentration is achieved by jointly traversing a laser beam and a camera across the volume of interest, resulting in a two-dimensional matrix of line measurements, which are used to plot planar contours. A sample measurement of a nuclei plume is presented for a high Reynolds number flow over a backward facing step. The flow was seeded with a relatively large, nominally mono-disperse, nuclei population injected at a point on the step model surface. Contour plots of nuclei concentration in the wake of the step are presented for three streamwise and five spanwise planes. For each measurement position images were acquired until a statistically significant number of nuclei were detected (minimum of 500 bubble detections) or until 200,000 images were acquired. With such limit, the minimum resolvable nuclei concentration was of the order of $\approx 0.01\text{mL}^{-1}$. The developed technique enabled successful characterization of an injected nuclei plume and provides another tool for rigorous modelling of nucleation in hydrodynamic facilities.

1 Introduction

Hydrodynamic cavitation is a complex phenomena controlled by a multitude of flow parameters, including the nuclei population. Recent model scale studies have quantified the influence of nuclei population on cavitation inception (Khoo *et al.*, 2021), as well as the dynamics of developed cavitation (Brandner, 2018). Therefore, to accurately model cavitation phenomena in hydrodynamic facilities, a thorough consideration of nuclei scaling, both in terms of concentration and size distribution, and transport is required.

The nuclei population typically consists of microbubbles and is characterised by a stochastic distribution, both in size and distribution within the flow volume. Characterisation of the nuclei size distribution has received considerable interest in the past and several techniques that cover various nuclei size ranges are in use in hydrodynamic facilities (e.g. Khoo *et al.*, 2020, Russell *et al.*, 2020). In the majority of hydrodynamic facilities the only control of the water nuclei content is through variation of dissolved gas concentration, such that the nuclei distribution within the flow volume may statistically be considered homogeneous. The Australian Maritime College (AMC) water tunnel is designed with a capability for rigorous control of the water nuclei content through complete nuclei elimination and artificial seeding, thus enabling experiments utilizing targeted seeding of specific areas within the flow. Such seeding can result in an inhomogeneous spatial distribution of the nuclei across the flow volume and a requirement to measure distribution is necessary.

Due to practical considerations, such as the range of measurable nuclei sizes, efficient acquisition of statistically significant datasets and ability to distinguish bubbles from particles, Mie-Scattering Imaging (MSI) (Russell *et al.*, 2020) has been selected as a base for development of a volumetric



nuclei measurement method described in this work. The scope of the present work is to develop an opto-mechanical system that will extend the MSI technique to a volumetric measurement. The performance of the system will be evaluated through a sample measurement of a nuclei plume dispersion for a backward facing step flow seeded through a point on the model surface.

2 Methodology

2.1 Experimental Setup

The experiments were performed in the AMC variable pressure water tunnel. The tunnel test section is 0.6×0.6 m square at the entrance, by 2.6 m long. The test section ceiling is horizontal, with the floor sloping 20 mm over the length to maintain a nominally constant speed and zero streamwise pressure gradient. The operating velocity and pressure are controlled independently, with ranges from 2 to 12 m/s and 4 to 400 kPa absolute respectively. The tunnel volume is 365 m^3 and is filled with demineralised water. Optical access is provided through acrylic windows on each side of the test section.

The test section absolute pressure is measured, depending on the value, from high or low range Siemens Sitransp absolute pressure transducers models 7MF4333-1FA02-2AB1 (range 0-130 kPa) and 7MF4333-1GA02-2AB1 (range 0-400 kPa) with estimated precision of 0.13 and 0.48 kPa respectively. The test section velocity is measured from the calibrated contraction differential pressure. Depending on the value, either a high or a low range Siemens Sitransp differential pressure transducers models 7MF4333-1DA02-2AB1-Z (range 0.25 kPa) and 7MF4333-1FA02-2AB1-Z (range 0-160 kPa) are used, with estimated precision of 0.007 and 0.018 m/s respectively. The water dissolved gas content is measured using an Endress+Hauser OxyMax WCOS 41 membrane sensor. Further details on the facility can be found in Brandner *et al.* (2006, 2007).

The experimental setup used for a sample measurement of the nuclei plume dispersion is identical to that used by Allan *et al.* (2022a) for characterization of cavitation inception in the wake of a two-dimensional BFS, and only a brief description will be provided here. The height of the model is, $h = 100$ mm, resulting with the expansion ratio $ER = H/(H - h) = 1.2$ and aspect ratio $AR = w/h \approx 6$. The model overall length is 820 mm and it consists of an upstream ramp and a 200 mm long horizontal section. The aft part of the model is equipped with a penetration 1.6 mm in diameter and located 205 mm upstream of the step, which is used as the injection port for nuclei seeding. A schematic of the BFS model is presented in figure 1.

The experiments were performed for a step height based Reynolds number, $Re = Uh/\nu = 1.2 \times 10^6$, where U is the velocity at the streamwise location of the step and ν is the kinematic viscosity of the water. Due to the effect of flow contraction induced by the presence of the step, U differs from the velocity measured at the test section entrance (U_t). Therefore, a correction based on the measurement of the pressure coefficient between the test section entrance and the streamwise position of the step (C_p) was applied, giving the equation derived using Bernoulli's principle, $Re = Re_t/\sqrt{1 + C_p}$. All the measurements were performed for the tunnel dissolved oxygen content between 2.75 and 3.25 ppm.

2.2 Nuclei Injection

The stochastic nature of the nuclei population, and thus the complexity of the nuclei concentration measurements, can be reduced by artificially seeding the water with a monodisperse nuclei population. To achieve this, a novel nuclei generation system, based on the use of high wall shear at the injection port as a mechanism for bubble generation, was employed.

A schematic of the system is presented in figure 2. Pressurized air is delivered to the injection port via a 358 mm long $25 \mu\text{m}$ diameter capillary, with the supply pressure regulated using a Proportion-Air QPV1TBNISZP10BRGAXL electronic regulator (range 0-10 bar) equipped with a Prevost $1 \mu\text{m}$

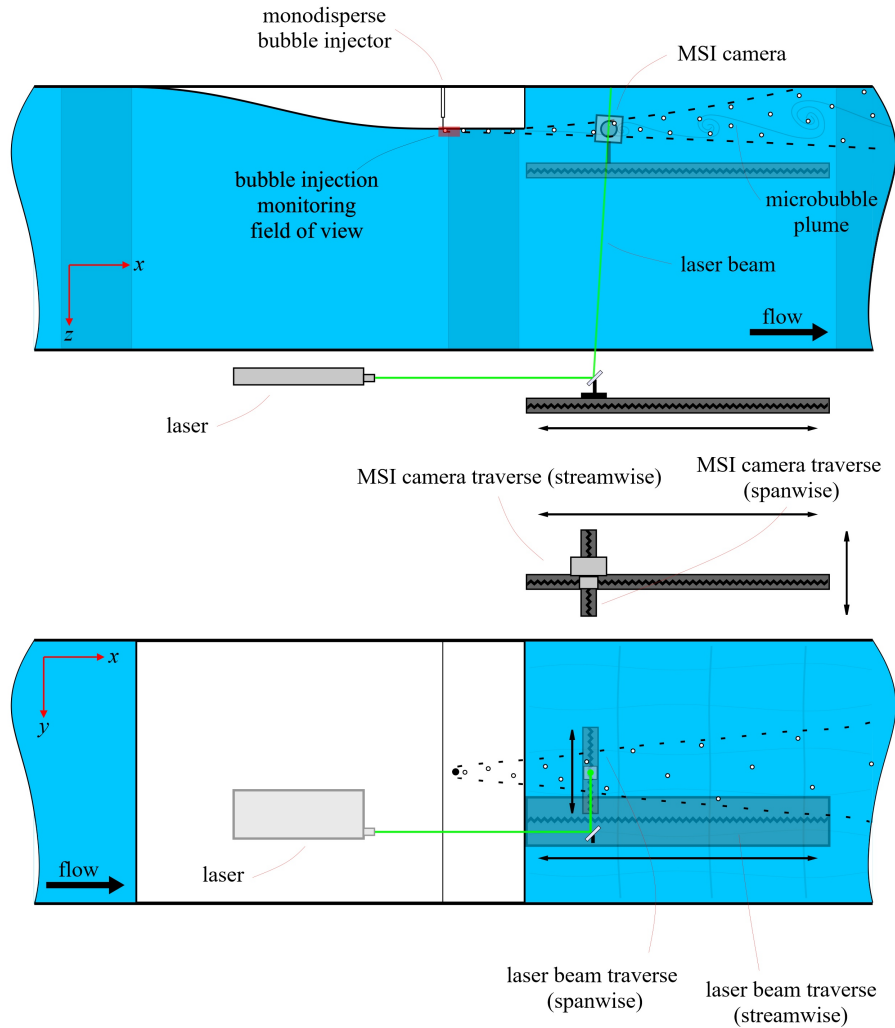


Figure 1. A schematic of the backward facing step (BFS) model and the optical system used for a sample measurement of nuclei dispersion. A side view is shown in the upper and bottom view in the lower portion of the figure. The area shaded with red in the side view represents the field of view of shadowgraphy measurements at the location of the nuclei injection port. The traverse system enables MSI measurements of nuclei in the wake of BFS from the step tip to 5.5 step heights downstream in the streamwise direction and a step height each side of the of the tunnel centreline in the spanwise direction.

air filter. The growing air volume undergoes coherent pinch-off similar to that in a microfluidic T-junction through a balance of increasing bubble drag, with wall shear overcoming bubble surface tension forces.

To examine and monitor the bubble generation process at the injection port, high-speed shadowgraphy of the injector port region (indicated with a red box in figure 2) was performed. The imaging setup utilized consists of a Photron Fastcam SA5 high-speed camera with a maximum resolution of 1024×1024 pixels equipped with a Nikon AF-D 200 mm f/4 Macro lens. The images were acquired at a reduced camera resolution of 256×64 pixels at 300,000 frames per second, with illumination provided from a single Scitech Constellation 120 continuous LED lamp.

A sample shadowgraphy image of a representative bubble train is shown in the inset in figure 2. The train consisted of bubbles ranging between 50 to 70 μm in diameter, with the bubble production rate, f_b , controlled by the differential pressure between the capillary inlet and the tunnel. For the purpose of current work an operating condition resulting in $f_b \approx 11$ kHz was selected. A more detailed description of the bubble generation method will be reported in a future publication.

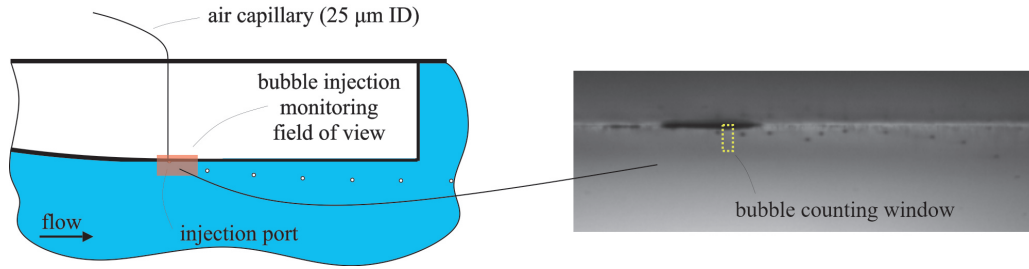


Figure 2. A schematic of the nuclei injection system consisting of a 25 μm diameter air capillary connected to the injection port flush to the BFS surface. Bubbles are produced via inertial pinch-off of the air volume at the injection port outlet due to the high velocity gradient and shear between the injector and free stream flows. A sample shadowgraph image of the bubble train at the outlet of the capillary tube is shown as an inset. A 3×11 pixel subsample, marked with yellow box, is used for the analysis of the bubble production rate.

2.3 Volumetric Mie-Scattering Imaging

In order to statistically characterise the dispersion of the injected nuclei plume, a volumetric nuclei measurement technique based on MSI has been developed. A schematic representation of the experimental setup used for spatial characterization of the nuclei plume is shown in figure 1.

The MSI measurements were acquired using a 48MP IO Industries Flare 48M30 CX high-speed CMOS camera equipped with a Nikon AF-S Nikkor 85 mm f/1.4 lens, located to the side of the test section. Bubbles were illuminated using an Ekspla NL204-SEH TEM₀₀ laser emitting 532 nm light with pulse frequency of up to 1 kHz and energy of 2 mJ per pulse. The laser was mounted horizontally below the tunnel test section, with the beam directed into the tunnel using two Thorlabs NB 1-K12 1" Nd:YAG mirrors. The beam entered the tunnel test section through an 80 mm thick acrylic window. To prevent burning of the acrylic window, the laser had to be operated at a lower power output, limiting the lower bound of detectable bubble size range. The beam was angled 7° from the vertical axis to prevent any reflected and refracted rays from overlapping the measurement beam. Accordingly, the camera was rotated so that the sensor long axis was parallel to the direction of the beam propagation. The camera was set with the sensor plane normal perpendicular to the beam so that the MSI measurement angle was 90° .

Spatial characterization is achieved by jointly traversing the laser beam and camera across the wake of the BFS. Position of the laser beam is adjusted by traversing the location of the two mirrors directing the beam into the tunnel. Streamwise positioning is achieved by mounting both mirrors on an Isel linear traverse with a 600 mm travel. Mechanical considerations limit the measurements to the range of position from the step up to 500 mm downstream. Spanwise positioning is achieved by mounting the mirror M2 on a Zaber linear traverse with a 200 mm travel attached to the streamwise traverse. This setup enables measurements 100 mm each side of the tunnel centreline. To maintain the camera streamwise position coincident with the position of the laser beam, as well as the camera defocussed distance, the camera was mounted to an identical traverse setup as the mirrors directing the beam.

Measurements of the nuclei spatial distribution were performed for three streamwise ($x - z$) and five spanwise ($y - z$) planes. Streamwise planes included the tunnel centre plane ($y = 0$) and planes located at $y = 0.2$ and $0.4h$. The increment between measurement points in the streamwise direction was set to $0.2h$. Spanwise distributions were obtained at the locations $x = 1, 2, 3, 4$ and $5h$ downstream of the step. The increment between measurement points in the spanwise direction was set to $0.2h$. As the laser beam is nominally aligned with the vertical axis, the vertical distribution is obtained along a continuous line, i.e. does not require incrementation. Due to symmetry of the nuclei plume, only one side was captured for both the streamwise and spanwise distributions.

For each measurement position images were acquired until a statistically significant number of bubbles was detected (minimum of 500 bubble detections). The required number of images varied

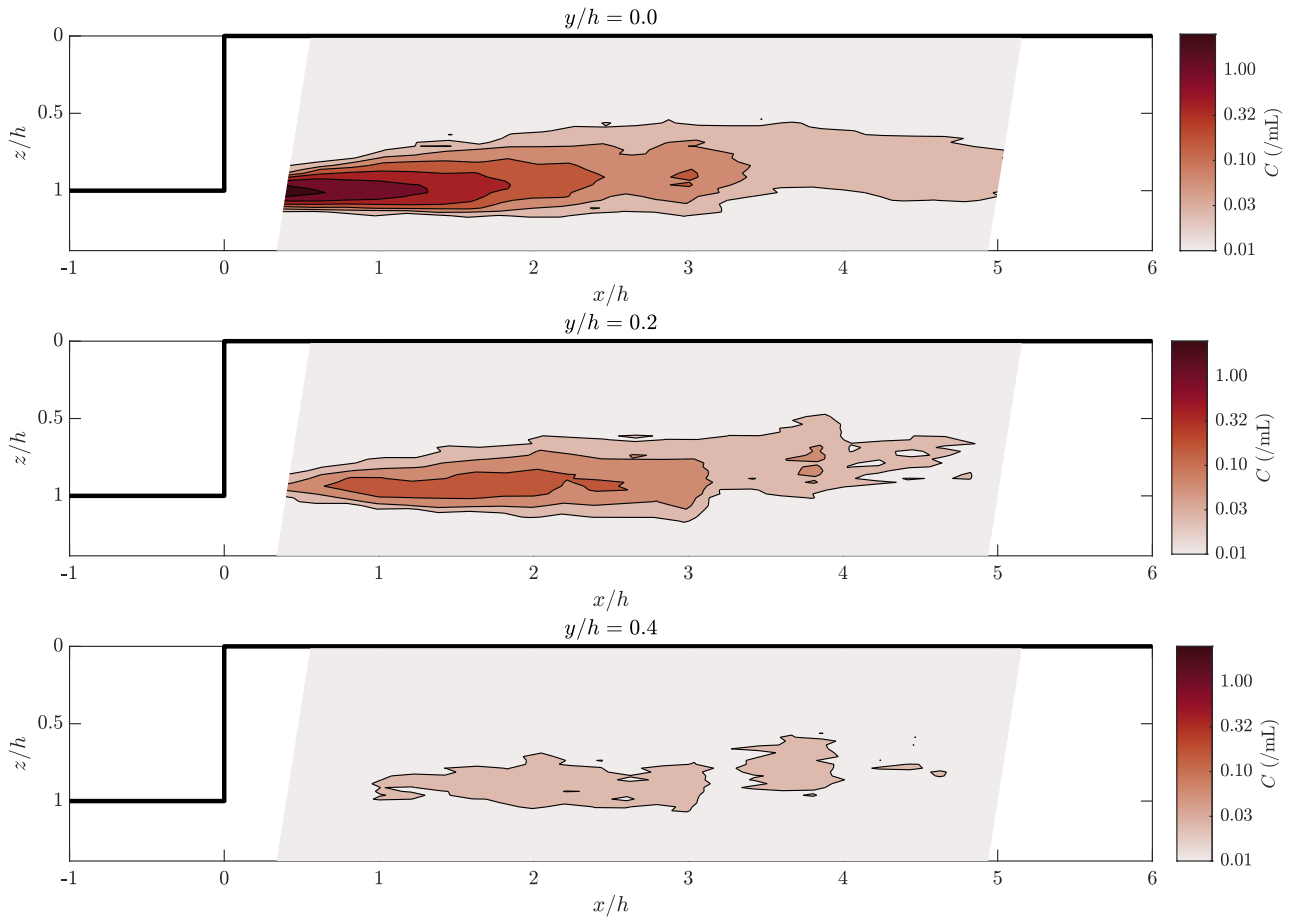


Figure 3. Contour plots of bubble concentration in the wake of a backward facing step for three stream-wise ($x-z$) planes at the spanwise locations $y = 0, 2$ and $4h$, obtained using volumetric nuclei measurement technique based on Mie-Scattering Imaging. Contours indicate the region with highest concentration at the tunnel centreline just downstream of the step. The bubble concentration reduces with increase in spanwise and streamwise distance from the tunnel centreline and step respectively. Note the logarithmic colour bar and spacing between the contours.

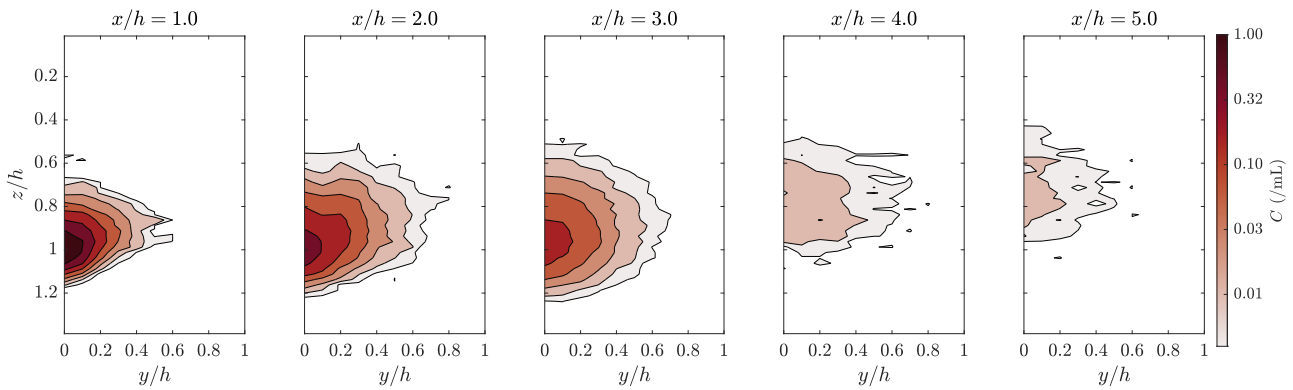


Figure 4. Contour plots of bubble concentration in the wake of a backward facing step for five spanwise ($y-z$) planes at the streamwise locations $x = 1, 2, 3, 4,$ and $5h$ downstream of the step, obtained using volumetric nuclei measurement technique based on Mie-Scattering Imaging. Note the logarithmic colour bar and spacing between the contours.

depending on bubble concentration across the plume, and accordingly samples of between 50,000 and 200,000 images were acquired. Given the sampling rate of 500 Hz, image acquisition for all the planes of interest took ≈ 20 hours. The MSI measurement calibration, data processing and analysis were performed using the method developed by Russell *et al.* (2020) and, for brevity, the details will not be provided here. A high-speed shadowgraphy dataset of bubble injection through the injector port was acquired every 10 minutes to monitor the bubble production rate.

3 Results

Contour plots of bubble volumetric concentration, C , for the streamwise planes are presented in figure 3 and for the spanwise planes in figure 4. Note that due to the wide range of concentration values, colour shading is logarithmically distributed. Nuclei are injected at a rate of $f_b = 11$ kHz at a position about 200 mm upstream of the step. The injected plume undergoes limited dispersion within the BFS wall boundary layer as it is advected along the BFS surface. The highest nuclei concentration, $C \approx 1 \text{ mL}^{-1}$, can be observed for the measurement point closest to the step and located at the tunnel $y = 0h$ plane (injection port plane). As nuclei are advected further downstream of the step, formation and increase in size of the shear layer structures promote dispersion of nuclei in the spanwise directions. This results in an increase in the extent of the nuclei plume in the $y - z$ plane, and consequently decrease in maximum concentration value in the $y = 0h$ plane. The maximum concentration value decreases about two orders of magnitude between the step and the most downstream measurement location.

The dispersion of the bubbly plume in spanwise directions is also evident in the contour plots of concentration distribution in the $y - z$ planes. It can be seen that for the two most downstream planes ($x = 4$ and $5h$) the plume appears to contract, however, this is a result of very low bubble concentration in this region, which would require acquiring an impractically large dataset to completely resolve.

4 Conclusions

A Mie-Scattering Imaging nuclei measurement technique has been successfully extended to characterise dispersion of nuclei within a flow volume. To demonstrate this capability, a sample measurement of a nuclei plume in the wake of a backward facing step seeded from a point on the model surface is presented. Utilizing the developed technique, detailed maps of nuclei concentration field in the wake of the step were obtained. For the presented sample, a low concentration limit, $C \approx 0.01 \text{ mL}^{-1}$, was observed, however, this limit can be extended by acquiring a larger dataset although at a significant time cost.

The described method requires detailed considerations of opto-mechanical setup that depend on the geometry of the experimental model, however, the basis for the volumetric MSI measurements presented here remains pertinent for any application. The technique described within this report represents an additional tool contributing to better understanding of the role of nuclei in cavitating flows.

Acknowledgements

The authors wish to acknowledge the assistance of Mr Robert Wrigley and Mr Steven Kent in carrying out the experiments. The authors wish to acknowledge the support of Australian Defence Science and Technology Group within the framework of the University of Tasmania collaborative work on Office of Naval Research 2017 US Multidisciplinary University Research Initiative (MURI) titled 'Predicting turbulent multi-phase flows with high-fidelity: a physics-based approach'.

References

- Allan, E.S.C., Barbaca, L., Russell, P.S., Venning, J.A., Pearce, B.W. and Brandner, P.A. 2022a, The influence of nucleation on cavitation inception in turbulent shear layers, *Proceedings of the 34th Symposium on Naval Hydrodynamics*
- Brandner, P.A., Lecoffre, Y. and Walker, G. J. 2006, Development of and Australian national facility for cavitation research, *Proceedings of the 6th International Symposium on Cavitation - CAV2006*.
- Brandner, P.A., Lecoffre, Y. and Walker, G. J. 2007, Design considerations in the development of a modern cavitation tunnel, *Proceedings of the 16th Australasian Fluid Mechanics Conference - 16AFMC*.
- Brandner, P.A. 2018, Microbubbles and cavitation: Microscales to Macroscales, *Proceedings of the 10th International Symposium on Cavitation - CAV2018*
- Khoo, M.T., Venning, J.A., Pearce, B.W. and Brandner, P.A. (2021), Nucleation and cavitation number effects on tip vortex cavitation dynamics and noise, *Experiments in Fluids*, 62(10):216
- Khoo, M.T., Venning, J.A., Pearce, B.W., Takahashi, K., Mori, T. and Brandner, P.A. 2020, Natural nuclei population dynamics in cavitation tunnels, *Experiments in Fluids*, 61:34
- Russell, P.S., Venning, J.A., Pearce, B.W. and Brandner, P.A. 2020, Calibration of Mie Scattering Imaging for microbubble measurement in hydrodynamic test facilities, *Experiments in Fluids*, 61 (4), 93.